Hindawi
Computational Intelligence and Neuroscience
Volume 2021, Article ID 5581637, 10 pages
https://doi.org/10.1155/2021/5581637

*Research Article*

# Artificial Neural Network-Based Method for Seismic Analysis of Concrete-Filled Steel Tube Arch Bridges

**Zhen Liu and Shibo Zhang**

*School of Management Science and Engineering, Shandong Technology and Business University, Yantai 264005, China*

Correspondence should be addressed to Zhen Liu; 201913693@sdtbu.edu.cn

Received 10 January 2021; Revised 16 March 2021; Accepted 27 March 2021; Published 7 April 2021

Academic Editor: José Alfredo Hernández-Pérez



Seismic analysis of concrete-filled steel tube (CFST) arch bridge based on finite element method is a time-consuming work. Especially when uncertainty of material and structural parameters are involved, the computational requirements may exceed the computational power of high performance computers. In this paper, a seismic analysis method of CFST arch bridge based on artificial neural network is presented. The ANN is trained by these seismic damage and corresponding sample parameters based on finite element analysis. In order to obtain more efficient training samples, a uniform design method is used to select sample parameters. By comparing the damage probabilities under different seismic intensities, it is found that the damage probabilities of the neural network method and the finite element method are basically the same. The method based on ANN can save a lot of computing time.

## 1. Introduction

Concrete-filled steel tubular arch bridge is the most common type of highway bridge, which plays an important role in the traffic network. When earthquakes struck, they are most likely to be damaged, and once they are damaged, they will seriously affect the transportation network in the area [1]. The dynamic response of CFST arch bridge under earthquake is very complex [2]. The seismic performance of the CFST arch bridge is influenced by various parameters (material and geometric parameters) [3, 4]. Therefore, it is very difficult to consider both efficiency and accuracy in seismic damage analysis of CFST arch bridges. The seismic damage prediction model based on finite element method will face huge computational complexity, and the amount of calculation increases exponentially with the increase of parameters. The introduction of some new technologies may lead to new solutions. The artificial neural network (ANN) may be the most useful method [5]. An ANN can be regarded as an organic combination of a large number of artificial neurons; it can be used to learn the inherent laws of data. Because this method is based on experiential data, ANNs can solve complex and nonlinear problems then replace traditional time-consuming and low-efficiency seismic damage analysis methods [6, 7]. A large number of studies have been made over the last ten years and ANNs have been used by many researchers in earthquake engineering. Some studies focus on seismic damage of highway bridges [8], considering material and geometric uncertainties. Some focus to predict the seismic performance of structures [9]. Furthermore, ANNs have estimated inelastic response of structures [10]. With the development of computer technology, ANNs are more widely used in earthquake damage prediction of bridges. However, the earthquake damage mechanism of CFST bridge is very complex, and there are many influencing factors. At present, there are few studies on seismic damage prediction of CFST bridges using ANNs.

Aiming at the difficulty of efficiency and accuracy in seismic analysis of CFST, an ANN-based seismic damage prediction method for CFST is proposed in this paper. The balance between the efficiency and accuracy of seismic evaluation can be found in this method to solve the seismic difficulty faced by CFST at this stage. This method takes the

calculated seismic damage data of CFST as training samples. The ANN is used to analyze samples in order to obtain the relationship between seismic damage and parameters of bridge-earthquake samples. The corresponding relationship is established in the ANN, and then the relationship can be used to predict the seismic damage of unknown bridge-earthquake samples.

## 2. Artificial Neural Network

The ANN can be used to predict the nonlinear systems of complex systems, and it is especially suitable for seismic damage identification of complex structures. The ANN composed of a large number of interconnected basic computing elements is similar to the working mechanism of the human brain. The network is composed of several layers: an input layer, hidden layers, and an output layer. ANNs can be divided into several types according to their structures. The multilayer radial basis function neural network (RBFNN), the multilayer perceptron (MLP), the probabilistic neural network (PNN), the learning vector quantization (LVQ), and the cascade correlation neural network (Cascor) are some useful neural network architectures [11].

In this paper, the RBFNN is used to predict earthquake damage. The Gaussian function is chosen as the activation function. Because of this function, RBFNN has better ability to deal with nonlinear data. The RBFNN has three layers as shown in Figure 1.

$x = [x_1, x_2, \ldots, x_n]$ $T \in R^n$ is the input vector, $W \in R^{\text{p.m}}$ is the output weight matrix, $y = [y_1, y_2, \ldots y_m]$ $T \in R^m$ is the output vector, $c_i$ is the data center value for the ith hidden node, $b_i$ is the bias for the ith node, $\varphi_i$ is the activation function for the ith hidden node, and $\|\bullet\|$ is the Euclidean distance for the input vector and the central vector. Due to space limits, the RBFNN would not be introduced detailed in this paper. More knowledge about the RBFNN can be found in neural network design [12].

The goal of the ANN is to build a historical data-based model in order to predict the output within a certain accuracy when the real output is unavailable. After training, the relationship between the input and the output data will be defined. In order to evaluate the prediction error of artificial neural network, the prediction error is defined as follows:

$$\text{MAE} = \frac{\sum_{i=1}^{k} \sum_{j=1}^{m} \left| Y_{ij} - T_{ij} \right|}{k \times m}, \tag{1}$$

$$\text{MAE} = \sqrt{\frac{\sum_{i=1}^{k} \sum_{j=1}^{m} \left( Y_{ij} - T_{ij} \right)^2}{k \cdot m}}, \tag{2}$$

where $Y_{ij}$ and $T_{ij}$ are the predicted value and the real value of the output, respectively; $k$ is the number of patterns in the test data and $m$ is the number of dimensions of the output vector.

## 3. Uniform Design Method

For the training of neural network, how to make the sample more representative is a very important problem. The methods of producing samples include traditional design, orthogonal design, and uniform design. When using the traditional design method, the number of design points will increase exponentially with the number of factors and the level of factors. Using the orthogonal design method, the computation time can be controlled in an acceptable range [13]. It is based on orthogonality to select some representative points from the comprehensive test. These representative points have the characteristics of "uniform dispersion and comparability." A problem contains 2 factors and 10 factor levels, which requires $10^2 = 100$ design points, less than the traditional design method. However, when there are many factors involved in the actual project, this method is not applicable.

The uniform design method (UDM) is especially suitable for the analysis of complex engineering problems, especially multifactor and multifactor engineering problems. Compared with the orthogonal design, the number of test points can be further reduced. Each level of each factor can only be done once. The UDM can significantly reduce the computing time. The uniform design is especially suitable for multifactor and multilevel experiments, and the system model is completely unknown. When a problem consists of 2 factors and 10 factor levels for each factor, only 10 design points are needed to use the UDM. The key of the UDM is the rules to ensure the uniformity [14]. Many discrepancy rules are used to estimate the uniformity of the UDM, such as discrete discrepancy and star discrepancy. The uniform design table (UDT) which makes the UDM easy to use is established based on construction rules, such as the Latin square rule. The UDT is regarded as a matrix which the number of the row is equal to the number of experiments and the number of the columns is equal to the number of factors. If the number of columns is more than the number of current factors, the accessional table which guides the selection of columns will be included in the UDT. The criterion of minimum discrepancy can be get using this selection rule. For example, 4-factor and 7-factor levels for each factor ($7^4$) are shown in Table 1 and its accessional table is shown in Table 2. In Table 2, the discrepancy is given according to the column and it can be found that the selected columns can be 1 and 3, but not the others when the number of current factors is 2. The minimum discrepancy can be obtained following this rule.

In this chapter, the key part is to determine the suitable samples according the UDM and the UDT.

Firstly, the factors should be determined. In this paper, only the material parameters are involved and no geometric parameters are involved due to the limitation of the number of samples. The distribution of uncertainty parameters is determined according to the related research [15, 16]. The probability distributions are assumed for each factor and the parameter ranges are corresponding to cumulative distributions from 0.05 to 0.95. The involved material parameters and their probability distributions are shown in Table 3.

Table 3 shows the means, coefficients of variation (COV), and ranges of material parameters. $E_{Q345}$, $E_{c40}$, and $E_{c50}$ are the elastic modulus of Q345 steel, C50 concrete, and C40 concrete, respectively; $f_{Q345}$, $f_{c40}$, and $f_{c50}$ are the

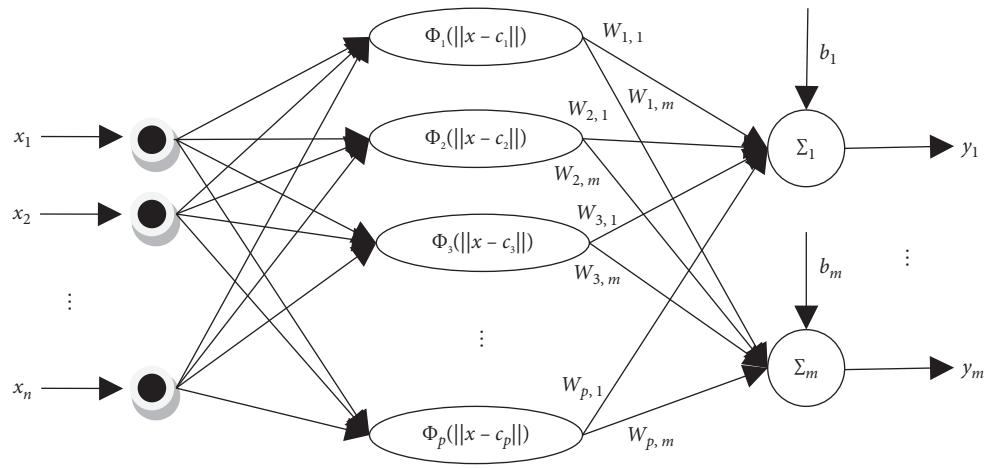


Figure 1: The structure of the RBFNN.

Table 1: Uniform design table for $7^4$.

| Point | Factor | | | |
|---|---|---|---|---|
| | 1 | 2 | 3 | 4 |
| 1 | 1 | 2 | 3 | 6 |
| 2 | 2 | 4 | 6 | 5 |
| 3 | 3 | 6 | 2 | 4 |
| 4 | 4 | 1 | 5 | 3 |
| 5 | 5 | 3 | 1 | 2 |
| 6 | 6 | 5 | 4 | 1 |
| 7 | 7 | 7 | 7 | 7 |

Table 2: Accessional table for $7^4$.

| $k$ | Column number | | | | Discrepancy |
|---|---|---|---|---|---|
| 2 | 1 | 3 | | | 0.2398 |
| 3 | 1 | 2 | 3 | | 0.3721 |
| 4 | 1 | 2 | 3 | 4 | 0.4760 |

Table 3: Material parameter uncertainties in bridge models.

| | Probability distribution | $\mu$ | COV | Range of variations |
|---|---|---|---|---|
| $E_{Q345}$ | Normal distribution | 206 GPa | 0.05 | 189–223 GPa |
| $f_{Q345}$ | Normal distribution | 345 MPa | 0.12 | 277–413 MPa |
| $E_{c50}$ | Normal distribution | 34.5 GPa | 0.05 | 31.7–37.3 GPa |
| $f_{c50}$ | Normal distribution | 32.4 MPa | 0.16 | 23.9–40.9 MPa |
| $\varepsilon_{c50}$ | Uniform distribution | $3.48e-3$ | 0.20 | $3.17–3.79e-3$ |
| $E_{c40}$ | Normal distribution | 32.5 GPa | 0.05 | 29.8–35.2 GPa |
| $f_{c40}$ | Normal distribution | 26.8 MPa | 0.16 | 19.7–33.9 MPa |
| $\varepsilon_{c40}$ | Uniform distribution | $3.53e-3$ | 0.20 | $3.21–3.85e-3$ |

reinforcement yield strength of Q345 steel, C40 concrete, and C50 concrete, respectively; $\varepsilon_{c40}$ and $\varepsilon_{c50}$ are the ultimate compressive strain of C40 concrete and C50 concrete, respectively.

The level number of each factor is assumed according to the expected number of samples. In this work, the level number is determined to be 20. Then, the range of each level can be calculated according to the parameter range and the level number of each factor. The $20^8$ UDT is used to design the sample according to the abovementioned analysis.

Once the $20^8$ UDT is determined, every column is a rearrangement of {1,2,3, . . .. . ., 20} which stands for the level of factor and every row is a true subset of {1,2,3, . . .. . ., 20} which corresponds to a sampling value of the factor. For example, if the number is 4, it represents that this parameter belongs to the fourth level and the value of this parameter is the average of maximum and minimum values of this level range.

## 4. Seismic Damage

In order to evaluate the seismic damage of the samples, an internal force and energy-based damage model which comes from Park-Ang, the double parameter failure criterion [17, 18], is used to quantify the seismic damage. The Park-Ang, the double parameter failure criterion, can be expressed as

$$D = \frac{\delta_M}{\delta_u} + \frac{\beta}{Q_y \delta_u} \int \mathrm{d}E, \tag{3}$$

where $D$ is a damage index according to the Park-Ang failure criterion; $\delta_u$ is the ultimate deformation of the component; $\delta_M$ is the maximum deformation under finite element analysis; $Q_y$ is the calculated yield strength; $dE$ is the incremental hysteretic energy.

In order to reflect the characteristics of CFST arch bridge, some modifications are made according to Park-Ang failure criterion. The adjusted seismic damage model is shown as follows:

Arch rib:

$$I_{ar} = \frac{\lambda_m}{\lambda_u} + \alpha \frac{\int E_h \mathrm{d}l}{\int (N_u \varepsilon_u + a M_u \varphi_u) \mathrm{d}l}. \tag{4}$$

Suspender:

$$I_{su} = \frac{\varepsilon_m}{\varepsilon_u} + \alpha \frac{\int E_h \mathrm{d}l}{\int N_u \varepsilon_u \mathrm{d}l}. \quad (5)$$

Beam:

$$I_{be} = \frac{\varepsilon_m}{\varepsilon_u} + \alpha \frac{\int E_h \mathrm{d}l}{\int M_u \varphi_u \mathrm{d}l}, \quad (6)$$

where $I_{ar}$, $I_{su}$, and $I_{be}$ are the damage index of arch rib member, suspender member, and beam member; $\lambda_m$ is the maximum ratio of axial force and bending moment of arch rib member cross-section in earthquake; $\lambda_u$ is the ultimate ratio of the axial force and bending moment of the cross-section of the arch rib member.; $\varepsilon_m$ is the maximum strain of one member cross-section in earthquake; $\varepsilon_u$ is the ultimate strain of one member cross-section; $N_u$ is the force bearing capacity of one member; $M_u$ is the ultimate bending moment of one member; $\varphi_u$ is the curvature of one member in the ultimate state; $E_h$ is the accumulated hysteretic energy of one member cross-section under the earthquake; $l$ is the length of one member; $\alpha$ is a coefficient; According to the suggestion of the paper [17], $\alpha$ is 0.139.

The seismic damage of each member of the bridge is different. One member contribution to the whole damage index is estimated by the accumulated hysteretic energy of the member under the earthquake and the contribution is expressed by the coefficient $w$. For example, the damage index of the whole suspender ($I_{su}$) is defined as follows:

$$\begin{cases} I_{su} = \sum (w_i)_{su} \left(I_j\right)_{su} \\ \left(w_j\right)_{su} = \left(E_j\right)_{su} / \sum \left(E_i\right)_{su} \end{cases}, \quad (7)$$

where $(w_j)_{su}$ is the weight value of one suspender member; $(I_j)_{su}$ is the damage index of the suspender member; $(E_j)_{su}$ is the accumulated hysteretic energy of the suspender member under earthquake; $\sum(E_j)_{su}$ is the accumulated hysteretic energy of the whole suspender members under earthquake.

According to the same rule, the damage index of the whole bridge can be defined as

$$I = I_{ar} w_{ar} + I_{su} w_{su} + I_{be} w_{be}. \quad (8)$$

The whole suspenders contribution to the whole bridge damage index can be defined as

$$w_{su} = \frac{E_{su}}{\left(E_{ar} + E_{su} + E_{be}\right)}, \quad (9)$$

where $I_{ar}$, $I_{su}$, and $I_{be}$ are the damage indexes of the whole arch ribs, suspenders, and beams; $W_{ar}$, $W_{su}$, and $W_{be}$ are the weight values of the whole arch ribs, suspenders, and beams; $E_{ar}$, $E_{su}$, and $E_{be}$ are the accumulated hysteretic energy of the whole arch ribs, suspenders, and beams under earthquake.

Through the analysis of internal force and displacement, the seismic damage model quantifies the seismic damage. The different seismic damage levels can be described and divided by the index damage. According to the paper [19], the range of each damage level can be determined as Table 4:

## 5. Bridge Samples and Ground Motion Samples

In order to predict the damage of CFST arch bridge by the ANN, a certain amount of training data is needed to train the ANN. To obtain these data, one CFST arch bridge case is needed. The detailed dimensions of the CFST arch bridges are shown in Figures 2 and 3. The material parameters of CFST arch bridge are determined by using the UDT and material parameter table. Using this method, 20 models of CFST arch bridge are established. The CFST main arch section is modeled using a fiber model. The beam element is used to simulate the main arch, the column, the longitudinal beam, and the beam. The link element is used to simulate the suspender. The 3-D FEA models are modeled in the ANSYS program and the model of the bridges is shown in Figure 4.

To obtain the response of the bridges, a set of 50 ground motion records are selected as samples. From the Pacific Earthquake Engineering Research Center (http://peer.berkeley.edu/), a sufficient number of strong ground motion records are available. In order to simulate the moderate and severe earthquakes, the records are selected from the ground motions with magnitudes in the range between 6.0 and 7.7. To make it more efficient, the near field effects are not considered and source to site distances of the records range from 10 to 200 km.

The magnitudes and distances distribution of the selected records is given in Figure 5. From Figure 5, it can be observed that the magnitudes and distances distribution of the records is relatively uniform in the selected range. The representativeness of records is very important for the accuracy of ANNs.

1000 groups of bridge-earthquake samples are formed by 50 groups of earthquake samples and 20 CFST arch bridge model samples. The results of the first ten samples are shown as Table 5. Due to space limitations, all calculations are not shown.

## 6. Numerical Tests

In order to test the efficiency and accuracy of the ANN-based method, the comparison between the results based on the FEA program and the results based on the ANN model is made in this chapter. To train the ANN model, a set of data is obtained from the FEA program.

Based on the nonlinear time history analysis, the results of every bridge components are obtained. Then, the damage indexes of every bridge can be calculated based on the results. After getting the damage indexes, a well-trained ANN model will be developed to predict the damage index based on the input data. The ANN model used in this paper is RBFNN. This ANN is especially suitable for complex nonlinear problems. The RBFNN is consisted of three different layers: the input layer, the hidden layer, and the output layer. The input layer is made up of 11 nodes which input 8 material parameters and 3 ground motion parameters. The output layer has only 1 node which outputs the

Table 4: Damage index range of bridge structure under different damage degrees.

| Damage level | Damage index range |
|---|---|
| No damage state | 0.00~0.10 |
| Slight damage state | 0.10~0.30 |
| Moderate damage state | 0.30~0.50 |
| Extensive damage state | 0.50~0.70 |
| Collapse damage state | 0.70~1.00 |

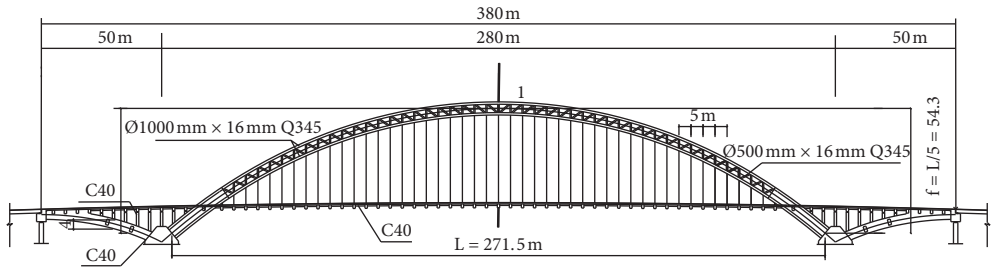


Figure 2: Elevation of the CFST arch bridge.

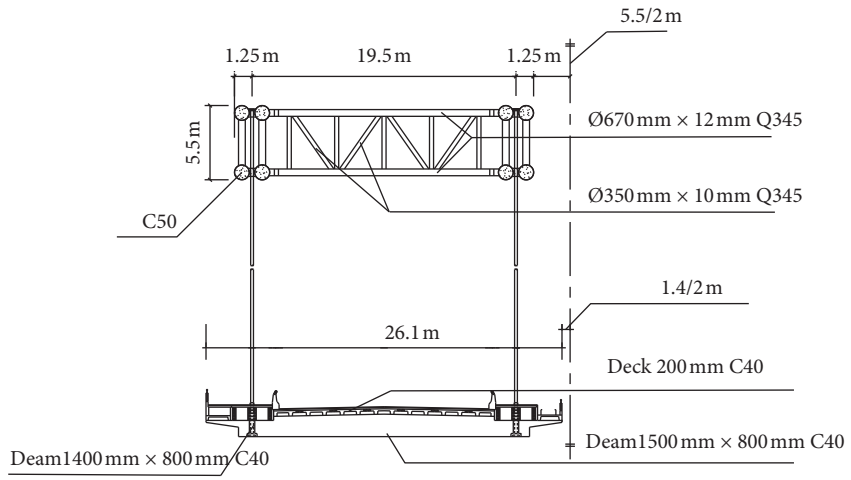


Figure 3: Transverse cross-section of the CFST arch bridge.

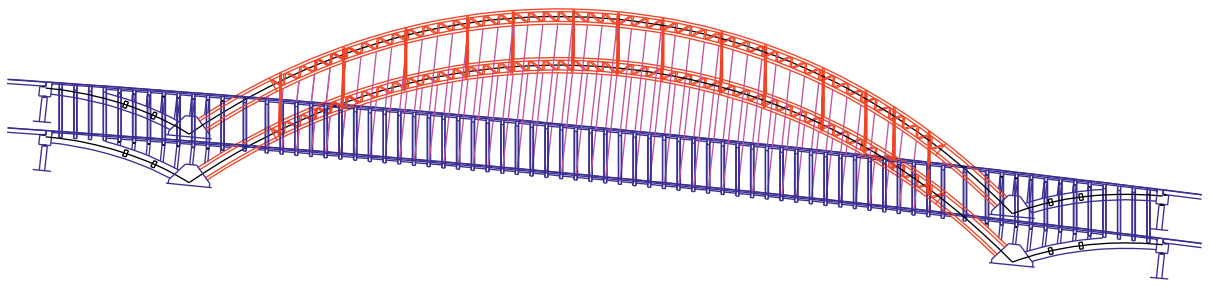

Figure 4: Three-dimensional finite element model of the CFST arch bridge using ANSYS.

damage index. The number of nodes in the hidden layer is variable. It is because the creating process of the multilayer RBFNN needs several attempts. The number of the nodes in the hidden layer is increased after each calculation, until the error of the multilayer RBFNN can meet the requirement which is set before calculation. The number of initial nodes of the hidden layer is 200. The default error is 1/1000. If the precision is not required, the number of nodes in the hidden

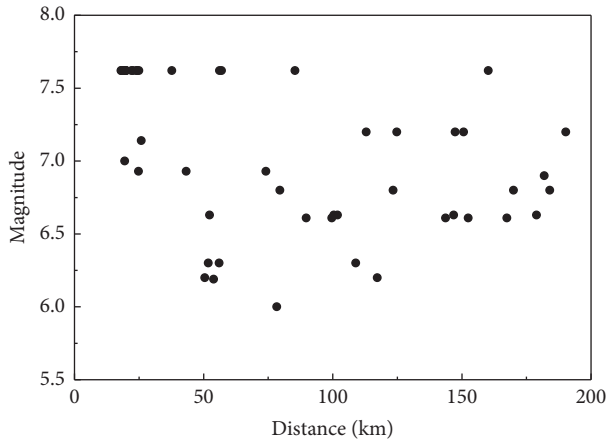


Figure 5: Moment magnitude and distance distribution for the selected 50 records.

Table 5: The damage index result.

| Magnitude | Rjb (km) | Vs30 (m/sec) | PGAx (g) | PGAy (g) | PGAz (g) | I |
|---|---|---|---|---|---|---|
| 6.610 | 89.370 | 813.480 | 0.020 | 0.015 | 0.010 | 0.184 |
| 6.190 | 53.890 | 116.350 | 0.043 | 0.065 | 0.016 | 0.186 |
| 6.930 | 43.060 | 133.110 | 0.274 | 0.220 | 0.083 | 0.241 |
| 6.930 | 24.520 | 215.540 | 0.084 | 0.072 | 0.027 | 0.186 |
| 6.930 | 74.040 | 873.100 | 0.079 | 0.079 | 0.029 | 0.183 |
| 7.620 | 24.960 | 235.130 | 0.147 | 0.117 | 0.091 | 0.203 |
| 7.620 | 19.930 | 538.690 | 0.173 | 0.227 | 0.125 | 0.201 |
| 7.620 | 19.070 | 277.500 | 0.159 | 0.153 | 0.165 | 0.248 |
| 7.620 | 19.370 | 492.260 | 0.302 | 0.639 | 0.123 | 0.337 |
| 7.620 | 24.100 | 442.150 | 0.142 | 0.182 | 0.079 | 0.220 |

layer will be increased until the number of hidden layer nodes is 1000. Because of this, the multilayer RBFNN architecture is different between each calculation. In order to train and test the multilayer RBFNN, the abovementioned method is used to regenerate 100 bridge samples and match them randomly with earthquake samples. The obtained earthquake-bridge samples are input into the FEA program to calculate seismic damage. Then, this part of the data is used to calculate MEA of the ANN prediction.

In order to optimize the input of ANN, the representation method of ground motion is discussed. Each ground motion sample can be defined in many ways, such as earthquake information and peak information. One is that earthquakes are defined by magnitude ($M$), fault distance ($D$), and shear wave velocity ($V$), and the other is that earthquakes are defined by the peak ground acceleration (PGA) of components in three directions of seismic waves. The two sets of data are used to train the ANN and the prediction error is obtained. The MEA of the PGA group is 0.010 and the MEA of the MDV group is 0.023. The conclusion that using PGA information as input is better than the MDV information can be obtained. Because of the low accuracy of prediction, the MDV-based RBFNN will not be involved in the following research.

The relationship between earthquake-bridge sample parameters and corresponding seismic damage index is very

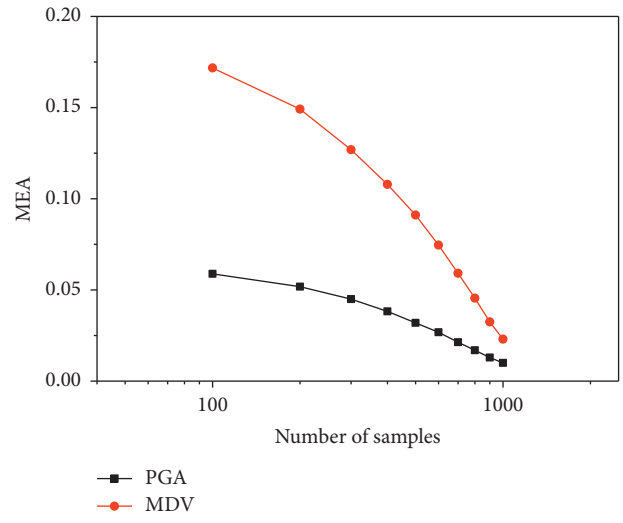


Figure 6: The relationship between MEA and the number of nodes in the hidden layer.

complex, and the corresponding structure of ANN used to predict seismic damage should also have a certain degree of complexity. But if the structure of ANN is too complex, it will lead to "over-fitting" of its prediction. In order to find the suitable structure of the ANN, different structures are discussed by using MDV group data. The difference between

Table 6: The relationship between seismic damage and earthquake intensity.

| | Direction | Interception | Slope | $\beta$ |
|---|---|---|---|---|
| FEA calculation | Along the bridge | −2.235 | 0.519 | 0.732 |
| | Transverse the bridge | −2.258 | 0.411 | 0.714 |
| | Vertical | −2.190 | 0.905 | 0.785 |
| Predicted value | Along the bridge | −2.254 | 0.542 | 0.803 |
| | Transverse the bridge | −2.247 | 0.435 | 0.788 |
| | Vertical | −2.217 | 0.877 | 0.871 |

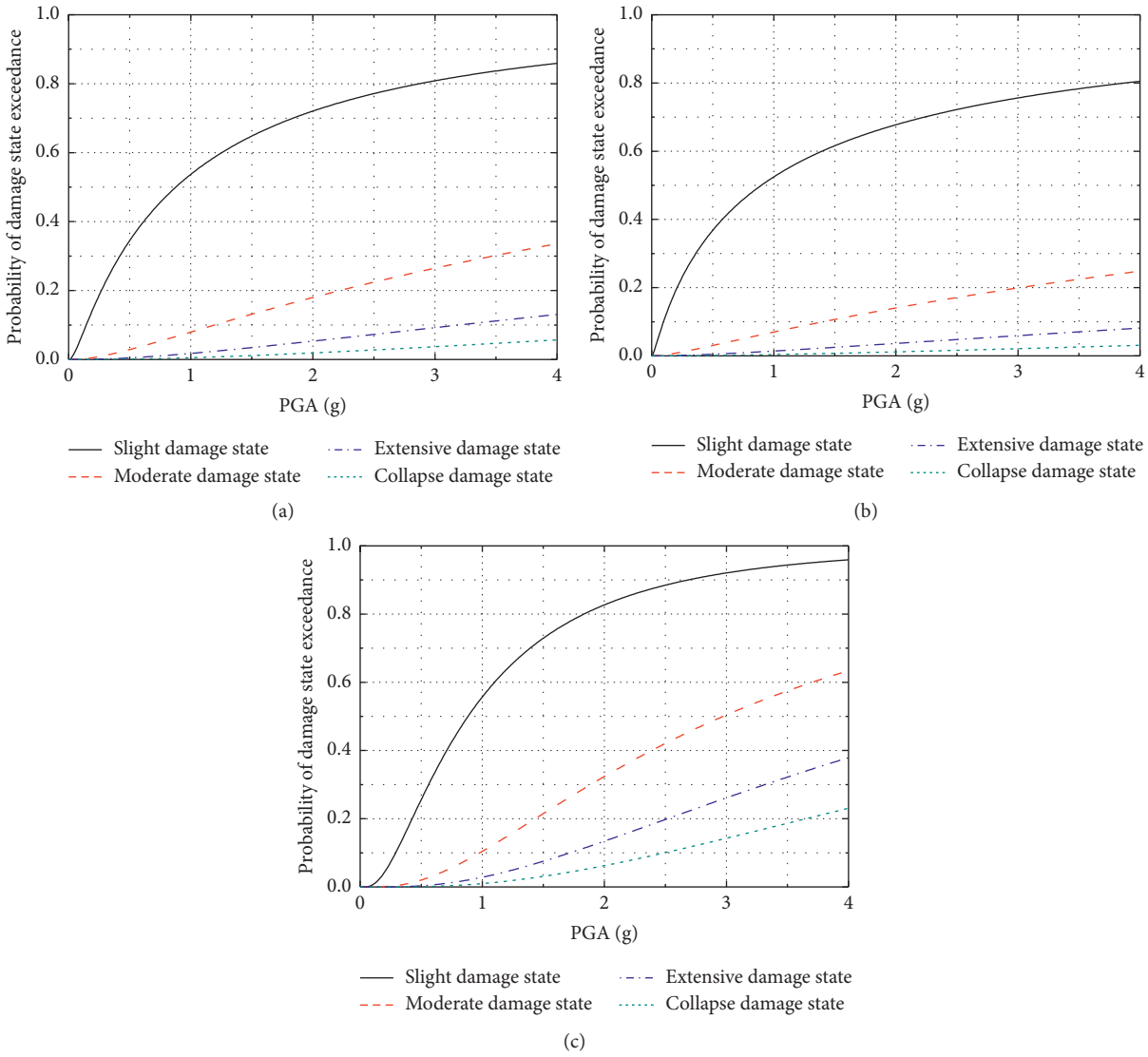


Figure 7: Fragility curves with PGA based on true values. (a) Along the bridge. (b) Transverse the bridge. (c) Vertical.

each ANN is only the number of neurons in the hidden layer. The number of neurons in the hidden layer and the prediction error (MEA) are shown as Figure 6.

From Figure 6, it can be found that with the increase of the number of neurons in the hidden layer, the prediction error of the ANN has been declining, and there is no obvious "over-fitting" problem. When the number of neurons reached 1000, the convergence speed of ANN and the decline trend of MEA slow down obviously. So, 1000 is defined as the maximum number of neurons in the hidden layer.

After determining the optimal ANN structure of the prediction model, it is necessary to systematically evaluate the prediction error and prediction speed of this model. Another 50 groups of ground motions are selected randomly from the PEER database as ground motion samples. From

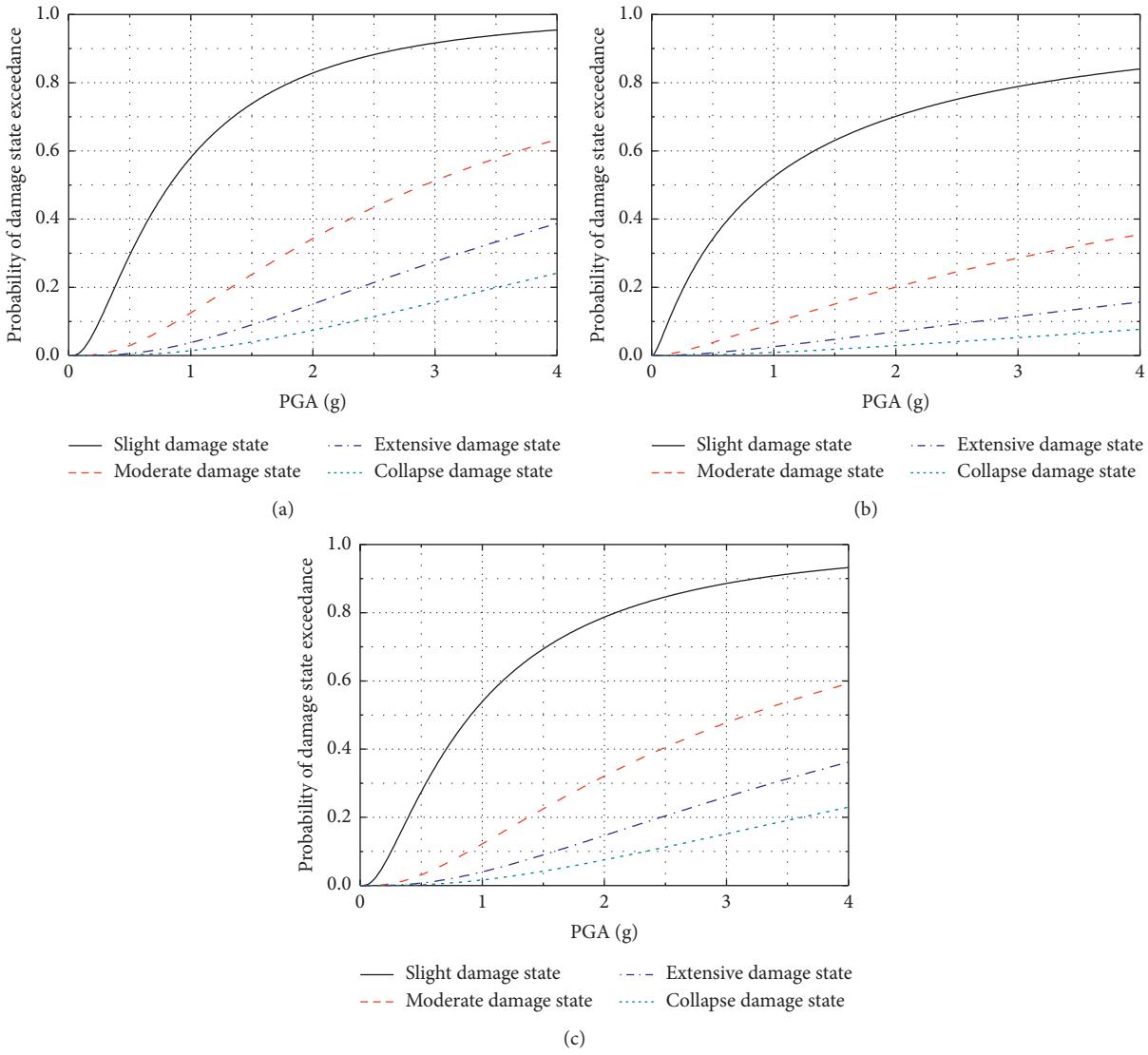


Figure 8: Fragility curves with PGA based on prediction values. (a) Along the bridge. (b) Transverse the bridge. (c) Vertical.

the bridge sample space in Table 3, 1000 samples are randomly generated. Because this group of samples is test samples, UDM method is not used to generate them. In order to form a bridge earthquake sample, the bridge sample and the earthquake sample are randomly paired. Then, the 1000 samples are input into the ANN-based model and the FEA program to calculate the seismic damage. The average relative error between the predicted value and the FEA calculation value is 3.21%, and the standard deviation is 0.0799. The relationships between earthquake intensity and seismic damage are obtained by using predicted values and FEA calculation values, respectively, and the relationship is shown in Table 6. Then, the corresponding seismic fragility curves can be obtained by using these relationships and these seismic fragility curves are shown in Figures 7 and 8.

Based on fragility curves, it is found that the difference between the predicted value and true value is very small. In order to quantitatively analyze this error, the earthquake is divided into four intensity levels, and the damage probability of the bridge under the four intensity levels is obtained by using the seismic vulnerability curve. Damage probabilities of predicted and true groups are listed in Table 7, and the maximum absolute error between the two groups is 3.99%. This shows that the model based on ANN can predict earthquake damage very accurately.

After the prediction accuracy of ANN model is obtained, the prediction speed of the model will be analyzed. On Intel (*R*) Core (TM) PC with 2.80 GHz i7CPU processor and 4 GB RAM, it takes 300 seconds to complete an RBFNN training. On the same PC, it takes more than 30 days to get these damage indexes by FEA program. It can be seen that the prediction model based on ANN can greatly reduce the calculation time of FEA program. Through the above-mentioned analysis of the accuracy and efficiency of the model, it can be concluded that the seismic damage prediction model based on ANN can effectively predict the seismic damage of the bridge.

Table 7: Damage probabilities of the predicted and true groups.

| | Direction | Earthquake intensity (g) | Probability of damage state exceedance (%) | | | |
|---|---|---|---|---|---|---|
| | | | Slight damage state | Moderate damage state | Extensive damage state | Collapse damage state |
| True value | Along the bridge | E1 (0.12) | 58.23 | 9.79 | 2.32 | 0.71 |
| | | E2 (0.20) | 71.58 | 17.60 | 5.17 | 1.84 |
| | | E3 (0.26) | 77.54 | 22.82 | 7.46 | 2.86 |
| | | E4 (0.34) | 82.82 | 28.97 | 10.52 | 4.34 |
| | Transverse the bridge | E1 (0.12) | 56.17 | 8.31 | 1.79 | 0.51 |
| | | E2 (0.20) | 67.34 | 13.78 | 3.54 | 1.14 |
| | | E3 (0.26) | 72.58 | 17.38 | 4.89 | 1.67 |
| | | E4 (0.34) | 77.48 | 21.62 | 6.67 | 2.43 |
| | Vertical | E1 (0.12) | 39.78 | 4.86 | 1.05 | 0.31 |
| | | E2 (0.20) | 62.93 | 14.25 | 4.27 | 1.58 |
| | | E3 (0.26) | 73.64 | 22.16 | 7.82 | 3.25 |
| | | E4 (0.34) | 82.68 | 32.37 | 13.39 | 6.22 |
| Predicted value | Along the bridge | E1 (0.12) | 56.75 | 11.54 | 3.33 | 1.21 |
| | | E2 (0.20) | 69.66 | 19.67 | 6.82 | 2.82 |
| | | E3 (0.26) | 75.55 | 24.94 | 9.47 | 4.17 |
| | | E4 (0.34) | 80.86 | 31.02 | 12.89 | 6.05 |
| | Transverse the bridge | E1 (0.12) | 56.36 | 10.86 | 2.99 | 1.05 |
| | | E2 (0.20) | 67.08 | 17.05 | 5.48 | 2.13 |
| | | E3 (0.26) | 72.14 | 20.97 | 7.28 | 2.99 |
| | | E4 (0.34) | 76.88 | 25.49 | 9.55 | 4.14 |
| | Vertical | E1 (0.12) | 40.02 | 6.50 | 1.78 | 0.64 |
| | | E2 (0.20) | 60.31 | 15.87 | 5.63 | 2.43 |
| | | E3 (0.26) | 70.04 | 23.10 | 9.310 | 4.38 |
| | | E4 (0.34) | 78.69 | 32.08 | 14.64 | 7.52 |
| Absolute error | Along the bridge | E1 (0.12) | −1.48 | 1.75 | 1.01 | 0.50 |
| | | E2 (0.20) | −1.92 | 2.07 | 1.65 | 0.98 |
| | | E3 (0.26) | −1.99 | 2.12 | 2.01 | 1.31 |
| | | E4 (0.34) | −1.96 | 2.05 | 2.37 | 1.71 |
| | Transverse the bridge | E1 (0.12) | 0.19 | 2.55 | 1.20 | 0.54 |
| | | E2 (0.20) | −0.26 | 3.27 | 1.94 | 0.99 |
| | | E3 (0.26) | −0.44 | 3.59 | 2.39 | 1.32 |
| | | E4 (0.34) | −0.60 | 3.87 | 2.88 | 1.71 |
| | Vertical | E1 (0.12) | 0.24 | 1.64 | 0.73 | 0.33 |
| | | E2 (0.20) | −2.62 | 1.62 | 1.36 | 0.85 |
| | | E3 (0.26) | −3.60 | 0.94 | 1.49 | 1.13 |
| | | E4 (0.34) | −3.99 | −0.29 | 1.25 | 1.30 |

Based on the calculation of a certain number of earthquake damage samples, the ANN model can effectively predict the earthquake damage of the bridge. When the seismic damage samples are enough, this method can well predict the seismic damage, thus to a certain extent, it can replace the finite element analysis and then quickly evaluate the seismic damage.

## 7. Conclusions

In this paper, a method of earthquake damage prediction based on artificial neural network is proposed, which replaces the time-consuming FEA method to a certain extent. This method can greatly reduce the amount of FEA calculation on the premise of ensuring the accuracy. Through certain training, the relationship between seismic parameters and seismic damage index of bridge is established. The average relative error is less than 3.21%. The seismic fragility curves show that there is no obvious difference between the predicted fragility curves and the fragility curves of the finite element program. Through the comparison of the earthquake damage probability of different intensities, it is found that the difference between the predicted earthquake damage probability and the FEA calculation earthquake damage probability is only less than 3.99%. This method only needs a small number of known samples and then can quickly and effectively predict the seismic damage of bridges.

## Data Availability

The data used to support the findings of this study have been deposited in the PEER database repository.

## Conflicts of Interest

The authors declare that they have no conflicts of interest.

## Acknowledgments

This work was supported by the National Natural Science Foundation Key Project of China (no. 51178080) and Doctoral Research Initiation Fund of Shandong Technology and Business University (no. BS201931). The authors would like to thank the Pacific Earthquake Engineering Research (PEER) Center for the earthquake data.

## References

[1] Q. Gao, Q. Ma, K. Cui, J. Li, and C. Xu, "Numerical investigation of the characteristics of the dynamic load allowance in a concrete-filled steel tube arch bridge subjected to moving vehicles," *Shock and Vibration*, vol. 2020, Article ID 8819137, 15 pages, 2020.

[2] H. Li, W. Luo, and J. Luo, "Seismic performance of steel box bridge piers with earthquake-resilient function," *Advances in Civil Engineering*, vol. 2020, Article ID 8877785, 24 pages, 2020.

[3] Y. Bai, S. Wang, and B. Mou, "Bi-directional seismic behavior of steel beam-column connections with outer annular stiffener," *Engineering Structures*, vol. 227, Article ID 111443, 2021.

[4] B. Mou, F. Zhao, and F. Wang, "Effect of reinforced concrete slab on the flexural behavior of composite beam to column joints: parameter study and evaluation formulae," *Journal of Constructional Steel Research*, vol. 176, Article ID 106425, 2021.

[5] Z. Liu and Z. Zhang, "Artificial neural network based method for seismic fragility analysis of steel frames," *KSCE Journal of Civil Engineering*, vol. 22, no. 2, pp. 708–717, 2018.

[6] J. Huo and L. Liu, "Evaluation method of multiobjective functions' combination and its application in hydrological model evaluation," *Computational Intelligence and Neuroscience*, vol. 2020, no. 2, p. 1, 2020.

[7] G. Hu, K. Wang, and Y. Peng, "Deep learning methods for underwater target feature extraction and recognition," *Computational Intelligence and Neuroscience*, vol. 2018, 2018.

[8] Y. Pang, X. Dang, and W. Yuan, "An artificial neural network based method for seismic fragility analysis of highway bridges," *Advances in Structural Engineering*, vol. 17, no. 3, pp. 413–428, 2014.

[9] M. S. Razzaghi and A. Mohebbi, "Predicting the seismic performance of cylindrical steel tanks using artificial neural networks (ann)," *Acta Polytechnica Hungarica*, vol. 8, no. 2, pp. 129–140, 2011.

[10] E. Bojórquez, J. Bojórquez, S. E. Ruiz, and A. Reyes-Salazar, "Prediction of inelastic response spectra using artificial neural networks," *Mathematical Problems in Engineering*, vol. 2012, pp. 1094–1099, 2012.

[11] M. Y. Rafiq, G. Bugmann, and D. J. Easterbrook, "Neural network design for engineering applications," *Computers & Structures*, vol. 79, no. 17, pp. 1541–1552, 2001.

[12] H. B. Demuth, M. H. Beale, O. De Jess, and M. T. Hagan, *Neural Network Design*, University of Colorado, Boulder, CO, USA, 2014.

[13] W. Gong, Z. Cai, and L. Jiang, "Enhancing the performance of differential evolution using orthogonal design method," *Applied Mathematics and Computation*, vol. 206, no. 1, pp. 56–69, 2008.

[14] W. X. Ren, S. E. Fang, and M. Y. Deng, "Response surface–based finite-element-model updating using structural static responses," *Journal of Engineering Mechanics*, vol. 137, no. 4, pp. 248–257, 2010.

[15] B. G. Nielson and R. DesRoches, "Seismic fragility methodology for highway bridges using a component level approach," *Earthquake Engineering & Structural Dynamics*, vol. 36, no. 6, pp. 823–839, 2007.

[16] Y. Pan, A. K. Agrawal, M. Ghosn, and S. Alampalli, "Seismic fragility of multispan simply supported steel highway bridges in New York State. I: bridge modeling, parametric analysis, and retrofit design," *Journal of Bridge Engineering*, vol. 15, no. 5, pp. 448–461, 2009.

[17] Y. J. Park and A. H. S. Ang, "Mechanistic seismic damage model for reinforced concrete," *Journal of Structural Engineering*, vol. 111, no. 4, pp. 722–739, 1985.

[18] Y. J. Park, A. H. S. Ang, and Y. K. Wen, "Seismic damage analysis of reinforced concrete buildings," *Journal of Structural Engineering*, vol. 111, no. 4, pp. 740–757, 1985.

[19] M. E. Rodriguez and D. Padilla, "A damage index for the seismic analysis of reinforced concrete members," *Journal of Earthquake Engineering*, vol. 13, no. 3, pp. 364–383, 2009.